

Supporting Information

Improved Efficiency of Single-Component Active Layer Photovoltaics by Optimizing Conjugated Diblock Copolymers

Dengke Shi^{b†}, Huabin Wang^{b†}, Hua Sun^a, Wenbo Yuan^b, Shifan Wang^{a*} and Wei Huang^{b*}

^a School of Material and Chemistry Engineering, Xuzhou University of Technology, Xuzhou, 221018, China

^b Key Laboratory of Flexible Electronics & Institute of Advanced Materials, Jiangsu National Synergistic Innovation Center for Advanced Materials, Nanjing Tech University, Nanjing 211816, China

* Corresponding authors: shifanwang@xzit.edu.cn (S. Wang)

iamwhuang@njtech.edu.cn (W. Huang)

†These authors contributed equally to this work.

EXPERIMENTAL

General methods. Reagents and chemicals were purchased from Aldrich, Acros and Fisher Scientific unless otherwise noted and used without further purification. P3HT-Br, BF8TBT and F8TBTSn were commercially available from Suna Tech Inc. ¹H NMR spectra were recorded using a Bruker Avance QNP 500 at 50°C. Chemical shifts are recorded in ppm (δ) in CDCl₃ with the internal references set to δ 7.250 ppm. Elemental analysis (C, H and N) was performed using a Vario EL III microanalyzer. M_n and M_w/M_n of values of polymers were measured with gel-permeation chromatography (GPC) with UV detector using chlorobenzene as eluent which was calibrated with polystyrene standards, at room temperature. Number-average (M_n) and Weight-average (M_w) of all the other polymers were determined by Agilent Technologies 1200 series GPC running in chlorobenzene at 80°C, using two PL mixed B columns in series, and calibrated against narrow polydispersity polystyrene standards. Preparative GPC utilized a Shimadzu recycling GPC system running in

chlorobenzene at 80 °C, using Agilent PL gel MIXED-D column, DGU-20A3 Degasser, LC-20A Pump, CTO-20A Column Oven and SPD-20A UV Detector. Differential scanning calorimetry (DSC) was performed on a NETZSCH DSC 200 PC unit within the temperature range of -50 to 350°C, heating at a rate of 10°C/min under N₂ atmosphere. Absorption spectra were recorded with Carry 400 UV/visible spectrometer. Cyclic voltammetry (CV) was measured on a CHI660D electrochemical workstation with a solution of 0.1 mol/L tetrabutylammonium hexafluorophosphate (Bu₄NPF₆) in acetonitrile, and the polymer film on a Pt plate as the working electrode, a platinum wire as auxiliary electrode, and an Ag wire as pseudo-reference electrode with ferrocenium-ferrocene (Fc⁺/Fc) as the internal standard. The LUMO and HOMO energy level were calculated using the following equations: $E_{\text{HOMO}} = -(E_{\text{OX}} - E_{\text{Fc}} + 4.8)$ eV and $E_{\text{LUMO}} = -(E_{\text{RED}} - E_{\text{Fc}} + 4.8)$ eV, where E_{OX} and E_{RED} were determined from the onset of the first potential of the oxidation and reduction curves, respectively, and E_{Fc} was taken as the half-wave potential of ferrocene. Atomic force microscopy (AFM) was conducted on SPA300HV in tapping mode using an SPI3800 controller, Seiko Instruments Industry, Co., Ltd. Grazing incidence wide angle X-ray scattering (GIWAXS) measurements were performed at beamline I07, Diamond Light Source, Harwell Campus, Didcot UK, using a Pilatus 2 M detector ($\lambda = 0.992 \text{ \AA}$) under a protective atmosphere to avoid beam damage.

Device Fabrication and Measurements The polymer/polymer blend solar cells have a structure of indium tin oxide (ITO)-coated glass substrate /PEDOT:PSS/active layer/LiF/Al. Poly(ethylenedioxythiophene):poly(styrenesulfonate)(PEDOT:PSS) (Baytron P4083) was firstly spin-coated on the pre-cleaned ITO substrate ($20 \Omega \square^{-1}$) to produce a 35-nm-thick anode buffer layer. The a 85 nm thick active layer with a concentration of 10 mg/ml in chlorobenzene solution was spin-coated onto the PEDOT:PSS layer. The samples were then transferred into a vacuum evaporator and a cathode including 1 nm of LiF and 100 nm Al was thermally deposited on top of the active layer to produce an active area of 0.12 cm² for each device. Devices with thermal annealing were carried out in a glove box at 150°C for 10 min. The illuminated current density-voltage (J - V) characteristics of the devices were measured

using a computer-controlled Keithley 236 source meter under 100 mW/cm² AM1.5G simulated solar light illumination. The light intensity was determined by a calibrated silicon diode with KG-5 visible color filter. The external quantum efficiency (EQE) of the devices was measured under short-circuit condition with a lock-in amplifier (SR830, Stanford Research System) at a chopping frequency of 280 Hz during illumination with the monochromatic light from a Xenon lamp.

Synthesis.

P3HT-b-F8TBT A mixture of P3HT-Br (9 k; GPC) (107 mg), K₂CO₃ (42 mg, 0.3 mmol) and Pd(PPh₃)₄ (8.7 mg, 0.007 mmol) were placed in a 10 mL Schlenk tube and the atmosphere was replaced with N₂. Toluene (8 mL) and H₂O (4 mL) were injected into the Schlenk tube, and then heated at 80 °C, 138 mg (0.15 mmol) of BF8TBT was dissolved in 2 mL of toluene, added to the Schlenk tube 3 times every half hour, and the reaction was continued overnight. After cooling to room temperature, the mixture was poured into methanol, and the resulting precipitate was filtered off and purified by subsequent Soxhlet extraction with methanol, acetone, ethyl acetate, and chloroform as final solvent. The chloroform fraction was precipitated from cold methanol again. After drying, a dark solid was collected. The Soxhlet extracted raw materials were then further purified on a preparative GPC by injection of 4 mL of concentrated chlorobenzene solution, fractions were manually collected. After evaporation of the chlorobenzene solvent, methanol was added, and the materials (BCP1-1 and BCP1-2) were collected as film and dried.

BCP1-1, ¹H NMR (500 MHz, CDCl₃), δ (ppm): 8.17 (d, H-Ar (PFTBTT-Block)), 7.93 (d, H-Ar (PFTBTT-Block)), 7.6-7.8 (m, H-Ar (PFTBTT-Block)), 7.50 (d, H-Ar (PFTBTT-Block)), 6.99 (s, Aryl-H(P3HT)), 2.80 (d, C-CH₂-C₅H₁₁), 2.12 (m; CH₂-C₇H₁₅), 1.74 (d, CH₂-CH₂-C₄H₉), 1.37 (m, CH₂-C₃H₆-CH₃), 1.14 (m; CH₂-C₅H₁₀-CH₃), 0.93 (t, CH₂-CH₃), 0.80 (m; C₇H₁₄-CH₃). GPC $M_n = 49.3$ kg/mol, $M_w = 57.2$ kg/mol, PDI = 1.19. EA found: C, 73.84; H, 7.81; N, 2.78.

BCP1-2, ¹H NMR (CDCl₃, 500 MHz) δ (ppm): 8.16 (d, H-Ar (PFTBTT-Block)), 7.93 (d, H-Ar (PFTBTT-Block)), 7.6-7.8 (m, H-Ar (PFTBTT-Block)), 7.50 (d, H-Ar (PFTBTT-Block)), 6.99 (s, Aryl-H(P3HT)), 2.80 (d, C-CH₂-C₅H₁₁), 2.10 (m; CH₂-

C₇H₁₅), 1.73(d, CH₂-CH₂-C₄H₉), 1.37 (m, CH₂-C₃H₆-CH₃), 1.15 (m; CH₂-C₅H₁₀-CH₃), 0.93(t, CH₂-CH₃), 0.89 (m; C₇H₁₄-CH₃). GPC $M_n = 24.7$ kg/mol, $M_w = 32.9$ kg/mol, PDI = 1.41. EA found: C, 73.73; H, 7.81; N, 2.70.

P3HT-b-TBTF8 A mixture of P3HT-Br (9 k; GPC) (107 mg) and Pd(PPh₃)₄(8.7 mg, 0.007 mmol) were placed in a 10 mL Schlenk tube and the atmosphere was replaced with N₂. Toluene (7 mL) and DMF (1 mL) were injected into the Schlenk tube, and then heated at 110 °C, 158 mg (0.15 mmol) of F8TBTSn was dissolved in 2 mL of toluene, added to the Schlenk tube 3 times every half hour, and the reaction was continued overnight. Post processing were synthesized using a procedure similar to that previously described. The materials (BCP2-1 and BCP2-2) were collected as film and dried.

BCP2-1, ¹H NMR (CDCl₃, 500 MHz) δ (ppm): 8.15(d, H-Ar (PFTBTT-Block)), 7.93 (d, H-Ar (PFTBTT-Block)), 7.6-7.8 (m, H-Ar (PFTBTT-Block)), 7.46 (d, H-Ar (PFTBTT-Block)), 6.98 (s, Aryl-H(P3HT)), 2.82 (d, C-CH₂-C₅H₁₁), 2.10 (m; CH₂-C₇H₁₅), 1.71(d, CH₂-CH₂-C₄H₉), 1.45 (m, CH₂-C₃H₆-CH₃), 1.14 (m; CH₂-C₅H₁₀-CH₃), 0.93(t, CH₂-CH₃), 0.81 (m; C₇H₁₄-CH₃). GPC $M_n = 64.6$ kg/mol, $M_w = 84.5$ kg/mol, PDI = 1.30. EA found: C, 73.91; H, 7.75; N, 2.83.

BCP2-2, ¹H NMR (CDCl₃, 500 MHz) δ (ppm): 8.15(d, H-Ar (PFTBTT-Block)), 7.92 (d, H-Ar (PFTBTT-Block)), 7.6-7.8 (m, H-Ar (PFTBTT-Block)), 7.47 (d, H-Ar (PFTBTT-Block)), 6.98 (s, Aryl-H(P3HT)), 2.80(d, C-CH₂-C₅H₁₁), 2.11 (m; CH₂-C₇H₁₅), 1.71(d, CH₂-CH₂-C₄H₉), 1.37 (m, CH₂-C₃H₆-CH₃), 1.14 (m; CH₂-C₅H₁₀-CH₃), 0.93(t, CH₂-CH₃), 0.81 (m; C₇H₁₄-CH₃). GPC $M_n = 32.9$ kg/mol, $M_w = 43.9$ kg/mol, PDI = 1.33. EA found: C,73.89; H, 7.78; N, 2.80.

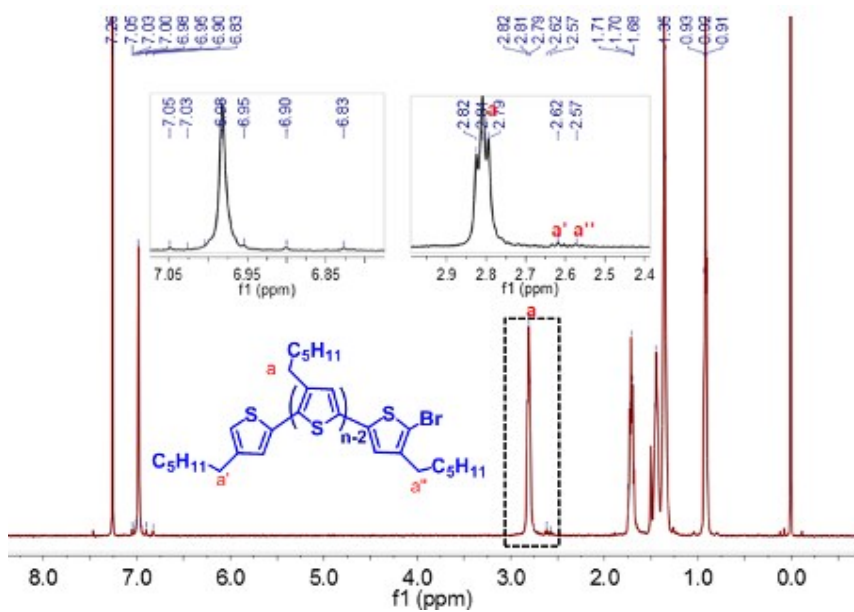
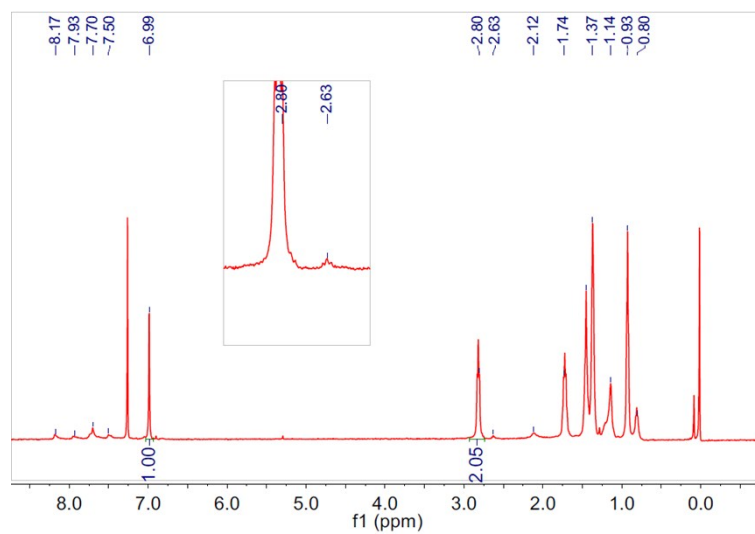


Figure S1 ¹H NMR spectra for P3HT



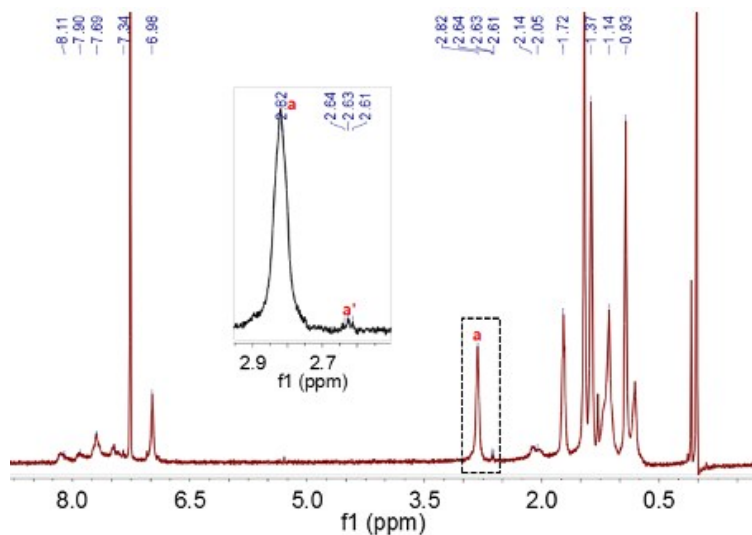


Figure S3 ^1H NMR spectra for BCP2-1 (top) and BCP2-2 (bottom).

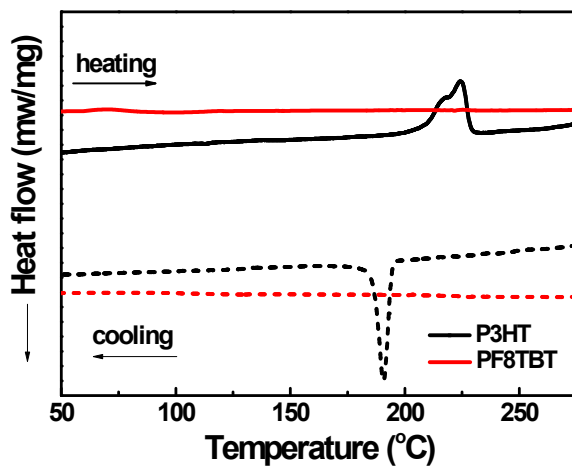


Figure S4 DSC curves of P3HT and PF8TBT

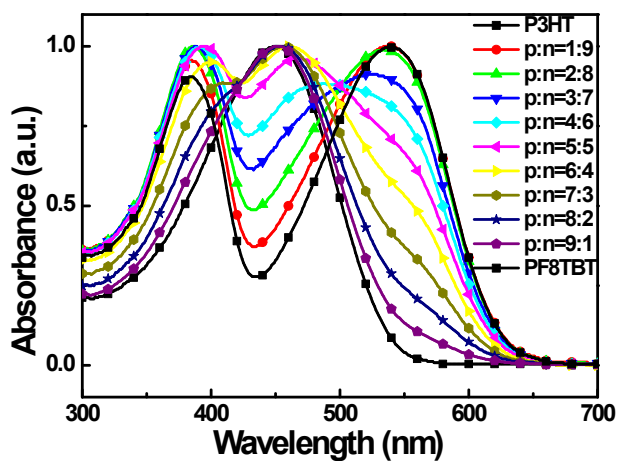


Figure S5 UV-Vis absorption spectra of P3HT, PF8TBT and their different proportions blended in chloroform solution

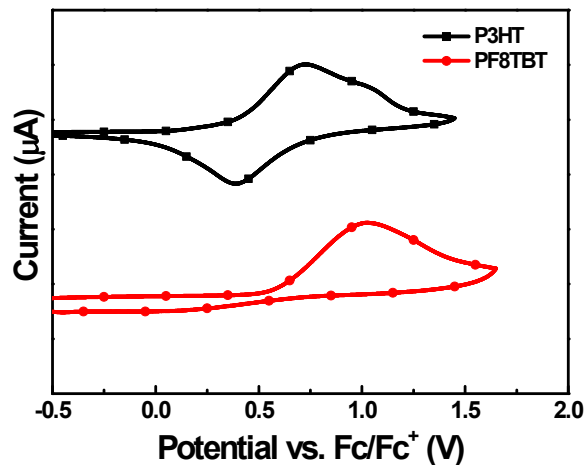


Figure S6 Cyclic voltammograms of P3HT and PF8TBT.

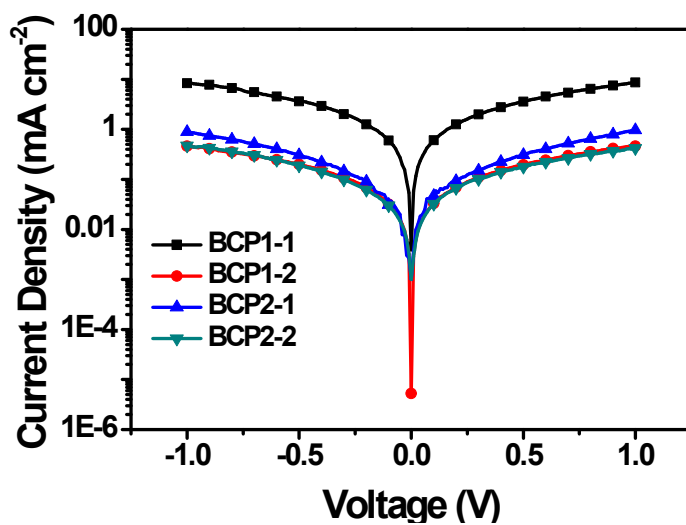


Figure S7 Dark J-V curves of photovoltaic devices that contained the D-A diblock copolymers.

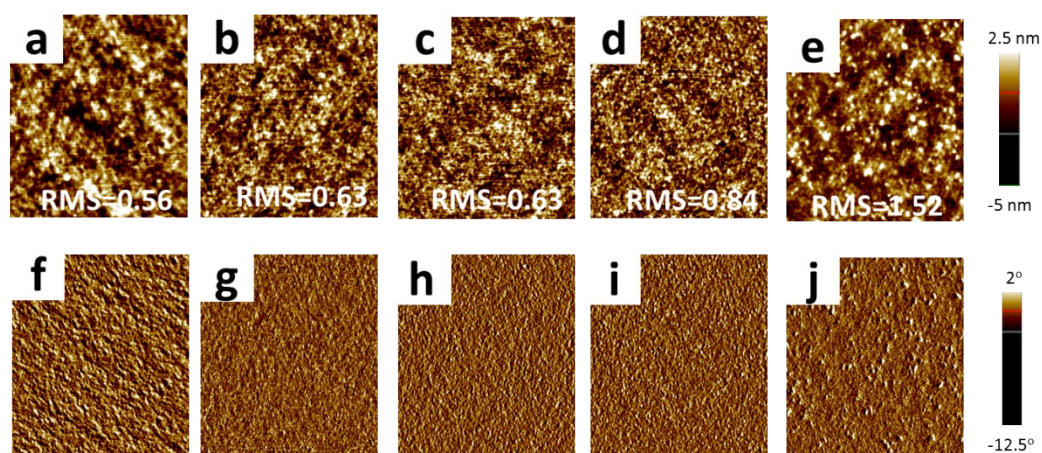


Figure S8 AFM height diagram (top) and phase diagram (bottom) in size $3\mu\text{m}\times 3\mu\text{m}$. (a, f) BCP2-1 as-cast, (b, g) BCP2-1 after 150°C annealed, (c, h) BCP2-2 as-cast, (d, i) BCP2-2 after 150°C annealed, and (e, j) BCP2-2 after 200°C annealed.

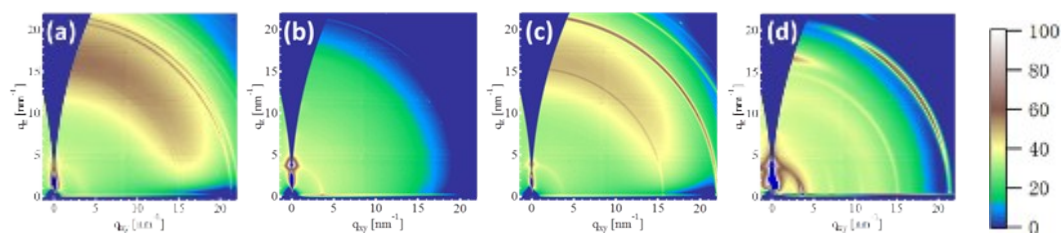


Figure S9 GIWASX images of (a) BCP2-1 as-cast, (b) BCP2-1 after 150°C annealed, (c) BCP2-2 as-cast, (d) BCP2-2 after 150°C annealed.

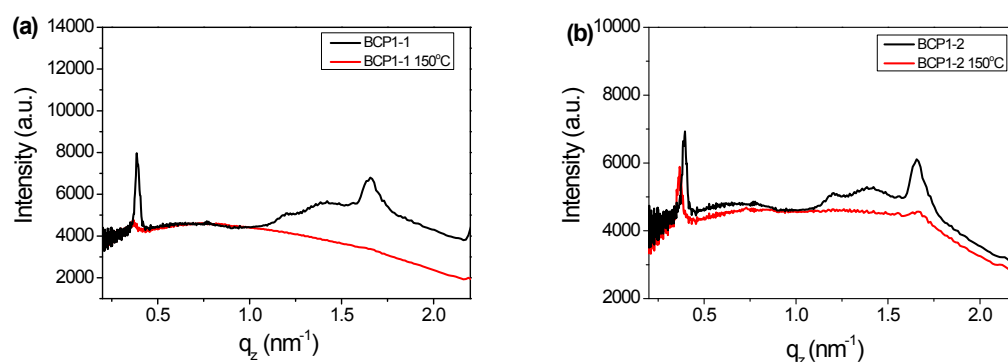


Figure S10 GIWASX 2D plots of (a) BCP1-1 and (b) BCP1-2.